An operando spectroscopic investigation of the Re2O7.2H2O adduct obtained by controlled hydration of Re2O7.

Xavier Sécordel, Shreya Nandi, Asma Tougerti, Sylvain Cristol, Jean-François Paul, Valérie Briois, Camille La Fontaine, Elise Berrier

Operando Spectroscopic Investigation of the $Re_2O_7.2H_2O$ Adduct obtained by Controlled Hydration of Re_2O_7.

Xavier Sécordel[1,2], Shreya Nandi[1], Asma Tougerti[1], Sylvain Cristol[1], Jean-François Paul[1], Valérie Briois[3], Camille La Fontaine[3], and Elise Berrier[1,⋆]

[1] *Univ. Lille, CNRS, Centrale Lille, ENSCL, Univ. Artois, UMR 8181 - UCCS - Unité de Catalyse et Chimie du Solide, F-59000 Lille, France*

[2] *Univ. Littoral Côte d'Opale, UR 4493, LPCA, IRenE, 145 Avenue Maurice Schumann, F-59140 Dunkerque, France*

[3] *Synchrotron SOLEIL, L'Orme des merisiers, Saint Aubin, F-91192 Gif-sur-Yvette*

[⋆] *Corresponding author: elise.berrier@univ-lille.fr*

Abstract

We provide here a comprehensive investigation spectroscopic of the controlled hydration of Re_2O_7 using Raman, Fourier-Transform Infrared (FTIR) and X-Rays Absorption (XAS) techniques in complement with *ab initio* modelling for confirming the spectral assignments. Hence, the Raman signature of $Re_2O_7.2H_2O$ was obtained, and the evolution kinetics was investigated to provide a detailed description of the hydration process.

1 Introduction

Solid rhenium heptoxide, Re_2O_7, looks like a yellow-greenish powder. Its use as catalyst has been reported in non-aqueous medium in alkene activation[1]. Its crystal structure, depicted for the first time in 1965 by Krebs and co-workers [2, 3, 4], is recalled in Fig. 1a). The solid Re_2O_7 is made of ReO_6 and ReO_4 units linked together by oxygen bridges to form a chain structure of double layers belonging to the $P2_12_12_1$ (or $\mathcal{D}_2^4$) space group. The unit cell parameters are the following: a = 12.508Å, b = 15.196Å and c = 5.448Å, while $\alpha = \beta = \gamma = 90^o$. The structure of Re_2O_7 can also be described as a polymeric lamellar organization based on cyclic Re_4O_{14} moieties retaining two Re atoms in tetrahedral coordination and two rhenium atoms in octahedral coordination (Fig. 1 b). The structure of Re_2O_7 embeds a wide variety of Re-O bond lengths and ReORe angles, so that the vibrational spectrum of the solid Re_2O_7 shows not less than 10 modes in the Re-O stretch region (798-1008 cm^{-1}) [5].

When submitted to ambient conditions, solid Re_2O_7 rapidly turns to a liquid drop of aqueous perrhenic acid solution in which the Re stands as a free, tetrahedrally coordinated perrhenate anion, ${ReO_4}^-{}_{aq.}$.

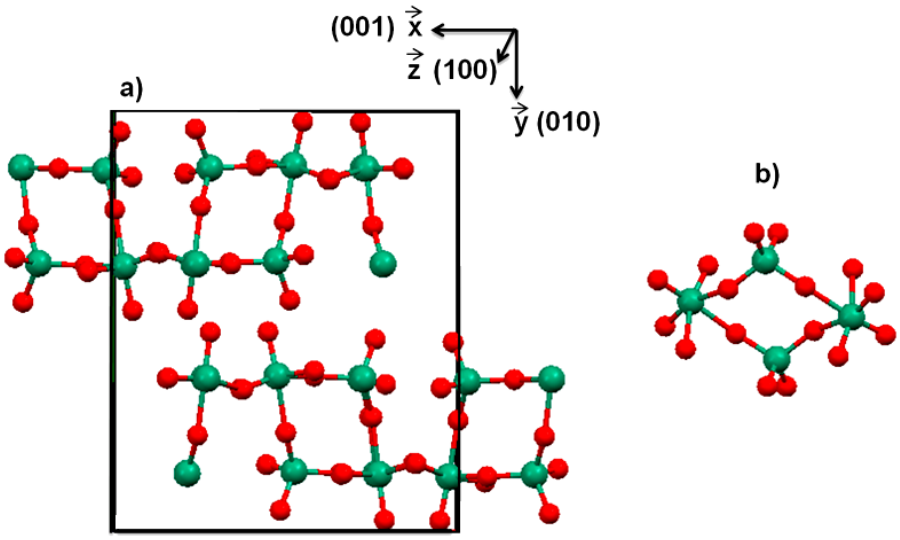

Figure 1: a) Structure of solid rhenium heptoxide and b) Cyclic arrangement of ReO_6 and ReO_4 building units; red: oxygen atoms, green: rhenium atoms

After impregnation of an oxide support by aqueous ${ReO_4}^-{}_{aq.}$, the oxorhenate phase remains as ${ReO_4}^-{}_{aq.}$ as long as the solid is subjected to moisture from air [6, 7, 8, 9]. Under dehydrated conditions, the supported oxorhenate phase consists of four-fold coordinated ReO_x monomers showing distorted structures [10, 11, 12, 13, 14]. Such supported phases have been successfully used for the methanol conversion to dimethoxymethane [15]. On the other hand, some studies have reported that under specific conditions of Re loading, catalyst preparation or atmosphere, original structures are yielded [16]. The presence of rhenium oxide oligomers is not likely, owing to the great volatility of Re_2O_7, but new molecular arrangements induced by a strong interaction with the support as well as the presence of water acting as ligand were proposed [17]. Examples of original water bonding in Re_2O_7-based materials were already presented and discussed in literature. A "solid perrhenic acid" formulated as $HReO_4$ can be prepared by concentration of an aqueous solution of Re_2O_7 over phosphoric anhydride [18], while recrystallization of $HReO_4$ from nitromethane yields the bis(aqua) adduct $Re_2O_7.2H_2O$ [19, 20, 21]. The structure of $Re_2O_7.2H_2O$ is rather unusual: it is made of one 4-fold coordinated rhenium atom (O-Re=O_3) bridged to one hexa-coordinated Re in a distorted octahedral geometry, as O-Re=$O_3(H_2O)_2$.

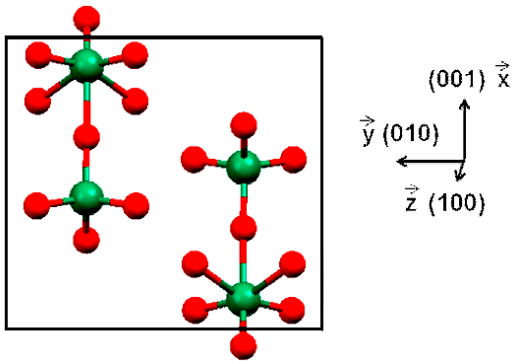

Figure 2: Structure of solid $Re_2O_7.2H_2O$ ReO_6 and ReO_4 building units are linked by an oxygen bridge (space group: P 21/m, unit cell parameters: a = 8.82Å, b = 8.89Å, c = 5.03Å, $\alpha = \beta = \gamma = 90^o$); red: oxygen atoms, green: rhenium atoms.

While both Raman and IR spectra of Re_2O_7 have been already discussed in the literature [5, 22], one can find only scarce spectroscopic characterization of $Re_2O_7.2H_2O$ [23]. Another crystalline form of perrhenic acid, $HReO_4.H_2O$, was also reported by Wltschek and co-workers [24]. The latter crystallizes into a scheelite-like structure (reference crystal formula: $CaWO_4$, $I4_1/a$, S_4, Z = 4) in which the tetrahedrally coordinated rhenium atoms are involved as ReO_4^- anions, the charge balance being due to the H_3O^+ counter ion. In other words, the Ca^{2+} cation from the aristotype $CaWO_4$ is replaced by H_3O^+ and the WO_4^- anion consists of ReO_4^-. In such a scheelite structure, the vibrations of the free ReO_4^- anion (4-fold coordinated) are expected to split because of the S_4 crystal site symmetry and the C_4^h factor-group effect, as Z = 4. As a result, the $\nu_1(A1)$, symmetric Re-O stretch vibration gives a single Raman-active mode (A_g) while the $\nu_3(F_2)$ antisymmetric one gives a doublet (E_g and B_g) of Raman-active vibrations. Hence, three Raman active components are expected between 750 and 1050 cm^{-1} [25].

Following a preliminary study of our group [23], the present work aims at carefully investigating the hydrated forms of Re_2O_7 in the solid-state. Such phases are targeted by means of a controlled hydration of Re_2O_7 under low partial pressure of water, while evaluating both the water uptake and the structural properties of the hydrated phases of Re_2O_7 in real time by following an *operando* approach.

2 Experimental

2.1 Operando Raman and In Situ IR Spectroscopies

25 mg of commercial Re_2O_7 crystalline powder (Alfa Aesar) were placed into a commercial Raman reaction chamber equipped with a flat quartz dome developed by Harrick Scientific[1] under argon in a glove box. The chamber was carefully closed using two 3-way valves, allowing a further bypass. After a cautious purge of all pipes at 65^{o}C under a dry helium flow (100 mL/min), a flow of helium at atmospheric pressure containing a partial pressure of water fine-tuned to 1350 Pa was allowed in the reactor at t = 0. The water was introduced by bubbling 20 mL/min He in a glass saturator equipped with a condenser circulating cooling liquid. The temperature on top of the condenser was carefully set to ensure a good control of the water partial pressure. Micro-Raman spectra were recorded *in situ* during the controlled hydration of the crystalline powder at 40^oC to prevent water condensation on the optical window, using the 514 nm line of an Ar^+ laser (laser power on the sample: 4 mW). A long working distance 50X microscope objective (Olympus) was used to both focus the excitation beam and collect the scattered light. The latter was passed through a confocal hole (150 µm) and analysed by a nitrogen-cooled charge coupled device (CCD) detector (Labram Infinity, Jobin Yvon). The products were subsequently analysed using a μ-gas chromatograph (SRA) equipped with a PoraPLOT U (Agilent) and a 5Å molecular sieve columns and thermal conductivity detector (TCD) detectors. The reactant and product carrier pipes were heated up to 75^{o}C to avoid any water condensation in the lines.

The same environmental chamber equipped with the Fourier-Transform Infrared (FTIR) dome and the Praying Mantis developed by Harrick Scientific was used for the Diffuse reflectance infrared Fourier transform spectroscopy (DRIFTS) experiments. DRIFT spectra of the catalyst surface were recorded with 4 cm^{-1} resolution using a Thermo 460 Protégé FTIR spectrometer equipped with a MCT detector.

[1] https://www.harricksci.com/ftir/accessories/group/Raman-High-Temperature-Reaction-Chamber

2.2 X-Ray Absorption Spectroscopy (XAS)

The Extended X-Ray Absorption Fine Structure (EXAFS) experiments were run at SOLEIL Synchrotron on the SAMBA beamline (Spectroscopies Applied to Materials Based on Absorption). The bending magnet radiation from the SOLEIL source was vertically collimated by a first cylindrical bent mirror onto the Si(111) fixed exit sagittally focusing double crystal monochromator. A second cylindrical bent mirror focused vertically the monochromatic beam at the sample position onto a spot of 200 x 300 μm^2. The X-rays grazing incidence of the mirrors was set at 4 mrad to reject harmonics. L_3 Re XAS data were collected in transmission mode using Oxford ionization chambers. In a glove box under argon, commercial Re_2O_7 crystal (Alfa Aesar) was diluted in boron nitride, pressed into a pellet and placed in the holder of a cryostat. The sample holder was carefully sealed using valves to avoid any contact of the sample with air during its transfer. The EXAFS spectrum of Re_2O_7 was recorded under secondary vacuum at 77 K to reduce the random motions due to thermal effects. After a cautious purge of all pipes and a warm-up of the sample to room temperature, a flow of He containing 500 ppm of water was allowed in the sample chamber. The crystalline structure of the sample was frequently checked using a fibred Raman apparatus, as described in a preliminary study demonstrating the relevance and feasibility of the setup. After 7 hours, the hydrated crystal was obtained. The sample environment was thus pumped, and the pellet was cooled down to 77 K, so that the recording conditions were identical for both samples.
The EXAFS oscillations $\chi(k)$ were extracted by subtraction of the baseline, $\mu_0(E)$, using the AUTOBK program as implemented in the Athena software. Briefly, the AUTOBK program makes a background approximation by a polynomial curve of third degree. The flexibility of the generated function is controlled by the number of nodes used (knots, points connecting two consecutive splines) which are defined by the low R components in the Fourier Transform spectra of the EXAFS.

3 Computational Details

3.1 Ab Initio EXAFS Calculation

Ab initio calculations of the EXAFS theoretical spectra were performed on Re_2O_7 using FEFF 6.013 [26]. This program is a self-consistent, real-space multiple-scattering code. It was used in this work to calculate the EXAFS signal by simulating the scattering of a photo-electron at Re L_3 edge along all scattering paths within a cluster of 149 atoms. The atomic potentials were built up thanks to the Muffin-Tin approximation, and the Hedin-Lundqvist model was used to compute the exchange energy. The experimental crystallographic structure obtained by Beyer *et al.* [19] was used to generate the atomic positions. The calculation of the scattering paths was done for radius cluster size inferior or equal to 7.5Å.

3.2 Ab Initio Vibrational Frequencies Calculation

The periodic density functional theory (DFT) calculations have been performed using the Vienna Ab initio Simulation Package (VASP) package. The PBE method has been used to compute exchange and correlation energy. PAW pseudo-potentials have been used to model the electron-ion interaction. The wave function is expanded on plane wave up to 550 eV and a 3X3X5 Γcentre k-point mesh has been used. The atom positions have been fully optimized starting from the crystallographic data for both structures. The cell parameters were kept fixed because of the lack of experimentally validated parameters for Re in the DFT approximation including London dispersion, namely the DFT+D method. The latter is however mandatory, as the cell parameters of Re_2O_7 are governed by inter-layers van der Waals interactions. In

the present case, we hence considered that less is more. The harmonic normal modes have been computed analytically, taking into account all the internal degrees of freedom. Except for rotation and translation modes, which computed values ranged from -20 to +10 cm^{-1} in Re_2O_7 and from -60 to +3 cm^{-1} in $Re_2O_7.2H_2O$, respectively, no imaginary frequencies were computed. The break condition for the ionic relaxation loop, known as the EDIFFG parameter in VASP, was set to 0.03 $eV.Å^{-1}$ and the EDIFF parameter was set to 10^{-6} for convergence and 10^{-9} for the linear response. The second derivatives of the total energy with respect to the ions' position were computed by VASP using density-functional-perturbation theory (DFPT) using considering that the low symmetry of $Re_2O_7.2H_2O$ is too low to substantiate the lowering of displacements by symmetry consideration.

4 Results

4.1 Operando Investigation of the Controlled Hydration of Re_2O_7

The controlled hydration of the rhenium heptoxide, Re_2O_7, was followed using operando Raman spectroscopy: a spectrum was collected every minute in order to get kinetic details of the reaction(s). Not less than 3 hydrated forms of Re_2O_7 were detected and their corresponding Raman signatures in the 750-1050 cm^{-1} region are presented in Fig. 3 b-d, together with the spectrum of Re_2O_7 corresponding to $t = 0$ *min* (Fig. 3 a). The spectrum presented in Fig. 3 d corresponds to the well-known $ReO_4{}^-{}_{aq.}$ form; note that at this final stage, the sample is in the liquid phase. The Raman signature shown in Fig. 3 c was difficult to detect, owing to its short lifetime[2]. It shows 3 Raman peaks in the displayed region, as would be expected for a scheelite structure. However, the split observed here does not fully respond to the expected one, namely, the split of ν_3 into a doublet and the holding of ν_1 as a singlet, and does not match the Raman spectra of other perrhenate compounds with scheelite structure like $NaReO_4$ [27]. Still, the observation of 2 symmetric modes suggests a transient structure involving water as ligand of a fraction of Re centres, maintaining octahedrally coordinated species while the crystal structure collapse, as was proposed in the case of a one-pot prepared Re/SiO_2 microporous catalyst prepared by our group [17]. On the other hand, the evolution from spectrum a) to spectrum b) could be easily monitored, as is shown in Fig 3, right. Indeed, we could observe a gradual and smooth transition from Re_2O_7 to another crystalline solid having a blue-grey colour, denoted as **B** in the following.

Looking more in detail at the spectrum of Re_2O_7 shown in Fig. 3a, one can observe 12 noticeable bands detected at 801, 834, 858, 913, 932, 956 (shoulder), 964, 966, 975, 979, 996 and 1011 cm^{-1} in the 750-1015 cm^{-1} range. Such a high number of modes is not surprising, giving the C_1 symmetry of Re_2O_7. Those modes are all related to the stretch vibration of either terminal $Re{=}O_t$ or bridging Re-O bonds. The three bands between 750 and 865 cm^{-1} were assigned by Wachs and co-workers to Re-O bands implying a Re atom in octahedral coordination, while the modes observed between 900 and 1010 cm^{-1} were related to 4-fold coordinated ReO_4 moieties [7, 13]. Our periodic DFT frequency calculations confirm that the band at 1011 cm^{-1} is reliably correlated to $\nu_s(Re^{\triangle}{=}O_t)$, the symmetric stretching mode of the terminal $Re{=}O_t$ double bond, in which the rhenium atom stands in tetrahedral coordination. On the other hand, our frequency calculation points out that the corresponding symmetric stretching mode of terminal $Re{=}O_t$ bond in which the Re stands in 6-fold coordination, $\nu_s(Re^{\square}{=}O_t)$, is responsible for the line at 979 cm^{-1}. The very intense mode at 996 cm^{-1} corresponds to symmetric stretch $Re{=}O_t$ vibrations in both 6-fold and 4-fold coordinated Re, with a very strong coupling between both moieties. The

[2]We could observe only one spectrum, shown in Fig. 3 c, with a poor signal-to-noise ratio.

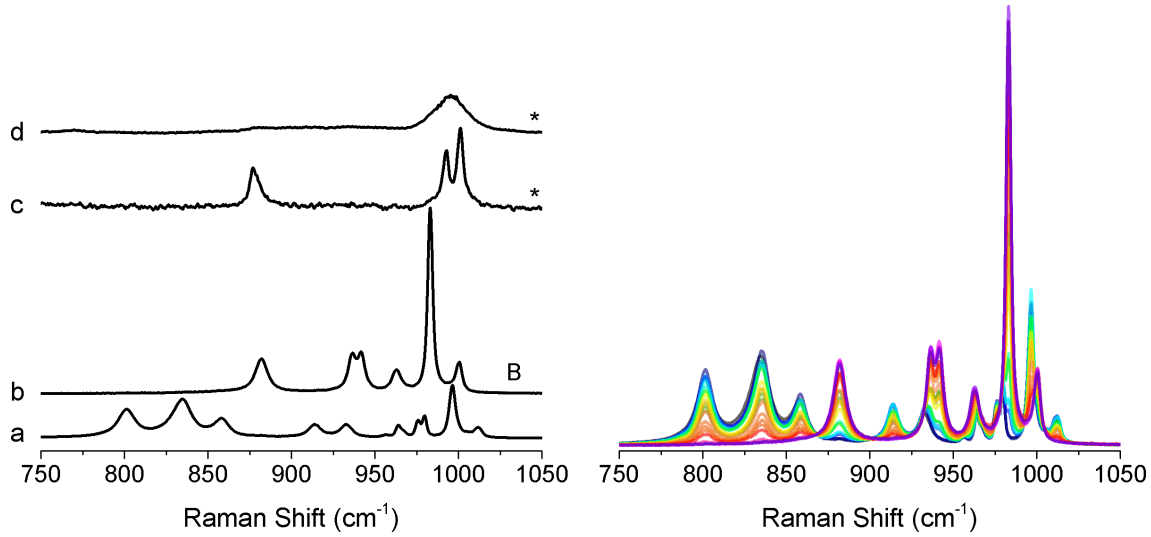

Figure 3: Left: spectra of all distinct phases observed during the controlled hydration of Re_2O_7 recorded at a) t=0; b) t=40 min; c) t∼60 min and d) t∼65 min; the spectra c and d have required a repositioning of the microscope objective for ensuring a proper focus on the sample. Right: detail of time-resolved spectral evolution from Re_2O_7 to **B**.

corresponding antisymmetric modes, namely $\nu_{as}(\mathrm{Re}^{\triangle}{=}\mathrm{O}_t)$ and $\nu_{as}(\mathrm{Re}^{\square}{=}\mathrm{O}_t)$ are expected at 986 and 956 cm^{-1}, respectively, while the computed frequencies of the strongly coupled modes involving both 4-fold and 6-fold coordinated Re centres are found to fall within the 967-977 cm^{-1} range.
Bridging single $\mathrm{Re}^{\triangle}$-O-$\mathrm{Re}^{\square}$ bonds are found along both x and y-axis in the structure of Re_2O_7 (see Fig. 1), giving rise to modes with computed frequencies at 931 and 900 cm^{-1}, respectively, plausibly related to the experimental lines at 932 and 913 cm^{-1}. Finally, three modes corresponding to the ensemble vibration of the Re_4O_4 in Re_4O_{14} tetramers are computed at 812, 840 and 860 cm^{-1}, corresponding to the experimental frequencies of 796, 830 and 853 cm^{-1}, respectively.

peak center (exp.) (cm^{-1})	rel. intensity %	calc. freq. (cm^{-1})	assignment
801	11.7	810	$\nu(Re-O)$ in Re_4O_4 cycle
834	15.1	844	$\nu(Re-O)$ in Re_4O_4 cycle
858	8.3	860	$\nu(Re-O)$ in Re_4O_4 cycle
913	5.8	900	$\nu_{(010),y}(Re-O-Re)$
932	5.7	931	$\nu_{(001),x}(Re-O-Re)$
956	1.8	956	$\nu_{as}(Re^{\square}{=}O_t)$
964,966	6.0	967,977	$\nu_{as}(Re^{\square,\triangle}{=}O_t)$
975	7.6	986	$\nu_{as}(Re^{\triangle}{=}O_t)$
979	9.4	1005	$\nu_{s}(Re^{\square}{=}O_t)$
996	22.1	1013	$\nu_{s}(Re^{\square,\triangle}{=}O_t)$
1011	5.0	1022	$\nu_{s}(Re^{\triangle}{=}O_t)$

Table 1: Raman peaks observed in Re_2O_7, calculated frequencies and tentative assignment; $Re^{\square}$=6-fold coordinated Re, $Re^{\triangle}$ = 4-fold coordinated Re

During the controlled hydration, all the modes of Re_2O_7 simultaneously decrease in intensity while new well-defined contributions due to another crystalline compound arise. The presence of obvious isosbestic points at 863 and 895 cm^{-1} suggests that (i) the Raman activities of the two compounds are comparable and (ii) only two species are involved in the process. After 30 minutes of hydration, the Raman signature

of **B** crystals becomes the majority, and subsequently the sole observed component. In the present experiment, **B** is stable until t=56 min. On the other hand, if no water is added in the atmosphere any more, *i.e.*, upon bypassing the saturator containing water, this compound is stable for at least 2 weeks. A similar experiment was run using D_2O instead of H_2O. The full spectra of **B** and its deuterated form, d-**B**, are shown in Fig. 4. The spectrum corresponding to d-**B**, presented in black in Fig. 4 b exhibits bands between 850 and 1000 cm^{-1} with almost no alteration in comparison with the one of **B**. On the other hand, the ν(OH) stretching region is severely shifted, as is expected for physisorbed water compared to physisorbed deuterium oxide. The vibrations observed between 150 and 400 cm^{-1} correspond to bending and rocking modes in ReO_4 and ReO_6 entities, and expected to show a significant degree of coupling. This is well-supported by the slight alteration of the peaks observed in the 150 and 400 cm^{-1} region between hydrated and deuterated compound. The high number of ν(Re-O) stretching modes, the nature of spectral modifications produced by isotope variation and the absence of ν(Re-OH) expected around 560 cm^{-1} suggest that compound **B** is $Re_2O_7.2H_2O$.

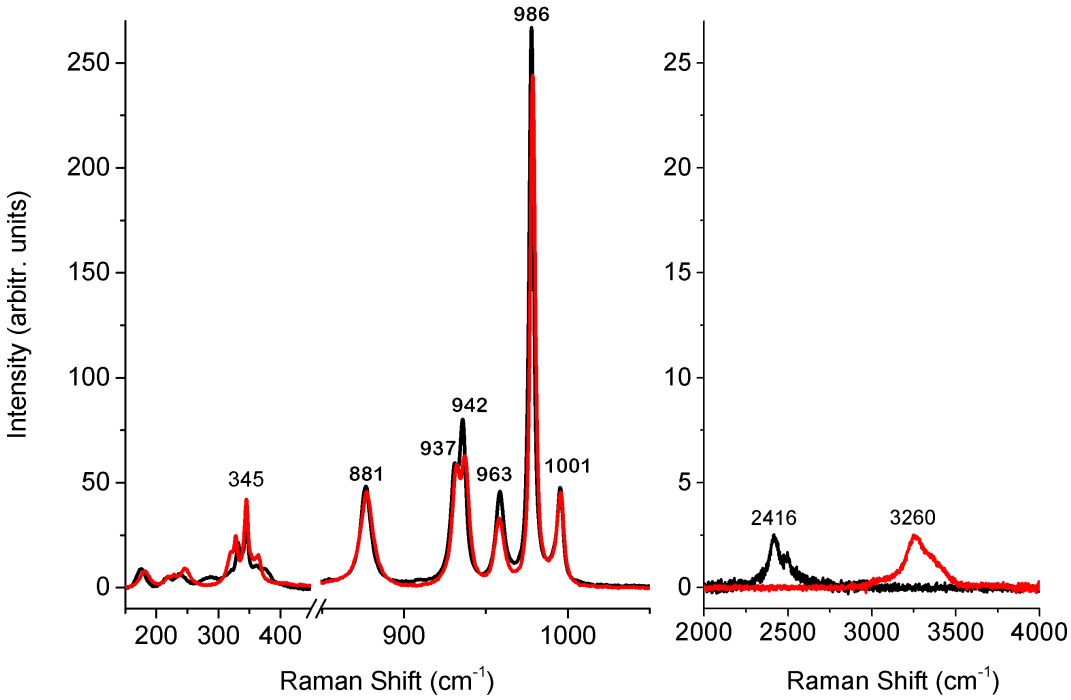

Figure 4: Raman spectra of $Re_2O_7.2H_2O$ (red line) and $Re_2O_7.2D_2O$ (black line)

As was made for Re_2O_7, a peak assignment of Re-O stretch vibrations supported by periodic DFT calculations is presented in Table 2. The coupling of the stretch vibration of terminal $Re^{\triangle}$=O and $Re^{\square}$=O is made even stronger, possibly because of the quasi-linear Re-O-Re bridging along (001) x-axis. As a result, only the $\nu_s(Re^{\triangle}=O_t)$ mode was found to be solely responsible for the 1001 cm^{-1} line (calculated frequency: 1013 cm^{-1}), while all the other stretch vibrations were found to result of a strong coupling between both $Re^{\square}$ and $Re^{\triangle}$. A remarkable new line arises at 881 cm^{-1} corresponding to an ensemble vibration involving both the bridging and terminal Re-O bonds along (001) axis. Noticeably, the modes related to Re_4O_4 cycles in Re_2O_7 have completely disappeared in $Re_2O_7.2H_2O$.

peak center (exp) (cm^{-1})	peak center (calc.) (cm^{-1})	assignment
881	895	$\nu_{(001),x}$(Re-O) in $Re^{\square}$-O$Re^{\triangle}$
937	945	$\nu_{as}(Re^{\square,\triangle}{=}O_t)$
942	959	$\nu_{as}(Re^{\square,\triangle}{=}O_t)$
963	978	$\nu_{as}(Re^{\square,\triangle}{=}O_t)$ in (yz) plan
983	990	$\nu_s(Re^{\square,\triangle}{=}O_t)$
1001	1013	$\nu_s(Re^{\triangle}{=}O_t)$

Table 2: Raman peaks observed in $Re_2O_7.2H_2O$ and tentative assignment

4.2 Confirmation of B Compound Identification by EXAFS and DFT Calculations

EXAFS experiments were at 77K run to confirm that the solid **B** is genuinely $Re_2O_7.2H_2O$. In general, one fits the Fourier transform parameters of the experimental spectrum for accessing the relevant parameters, neighbouring back-scatterer atoms and distances. However, in our case, the high contribution of the multiple backscattering paths mechanically increases the number of parameters to be implemented in the fitting process. As a result, the required number of parameters exceeds the number of independent variables, thus a comparison of theoretical and experimental spectra was preferred to a more usual spectral fitting approach. Based on the $Re_2O_7.2H_2O$ hypothesis, the theoretical EXAFS spectrum of $Re_2O_7.2H_2O$ was obtained by summing the contributions of the two non-equivalent rhenium sites following a gradual introduction of the backscattering paths, as is illustrated in Fig. 5.

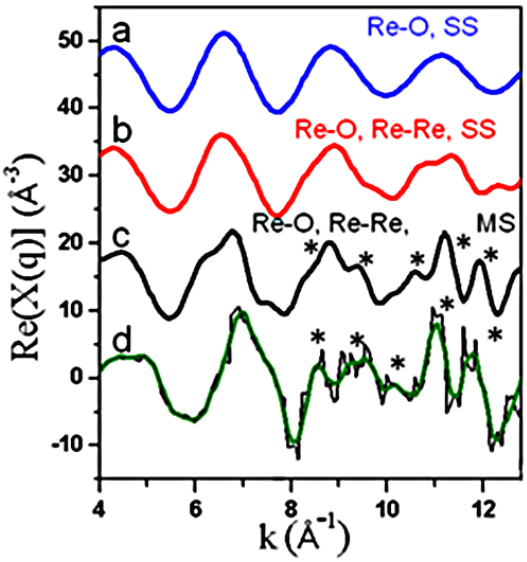

Figure 5: k^3-weighted Re L_3-edge theoretical EXAFS spectra of $Re_2O_7.2H_2O$ calculated by considering (a) only Re-O simple backscattering paths (blue), (b) Re-Re and Re-O simple backscattering paths (red), (c) sum of Re-O and Re-Re multiple scattering paths (black), (d) sum of Re-O and Re-Re multiple and simple scattering paths (green) plotted together with the experimental spectrum (black); colour online

The experimental spectrum, displayed in k space, is shown as a black line in Fig. 5 d. The theoretical spectrum, displayed as a green line in Fig. 5 d, was built according to the following sequence: at first, only the oxygen shell was considered (Fig. 5 a). Simple backscattering paths (SS) and multiple backscattering (MS) due to the Re shell were then introduced in the calculation (Fig. 5 b and c, respectively). Eventually, the global sum of all contributions is presented in Fig. 5 d. As long as only the oxygen shell is considered, the spectrum features a single oscillation without any beat pattern. The introduction of multiple backscattering paths was essential in reproducing correctly the experimental spectrum. Noticeably, the beat patterns in the 10 $Å^{-1}$-12 $Å^{-1}$ region, in which the Re contribution is maximal, are particularly well reproduced, confirming that the structure of the hydrated compound is $Re_2O_7.2H_2O$.

5 Discussion: Investigation of the Re_2O_7 to $Re_2O_7.2H_2O$ Reaction

Besides the identification of hydrated phases, the experimental protocol we have applied also makes it possible to monitor the Re_2O_7 to $Re_2O_7.2H_2O$ phase transition process. The presence of clear isosbestic points in the Raman spectra (see Fig. 3) as well as a covariance analysis shown in Fig. 6 suggest that only two components are involved in this phase transition.

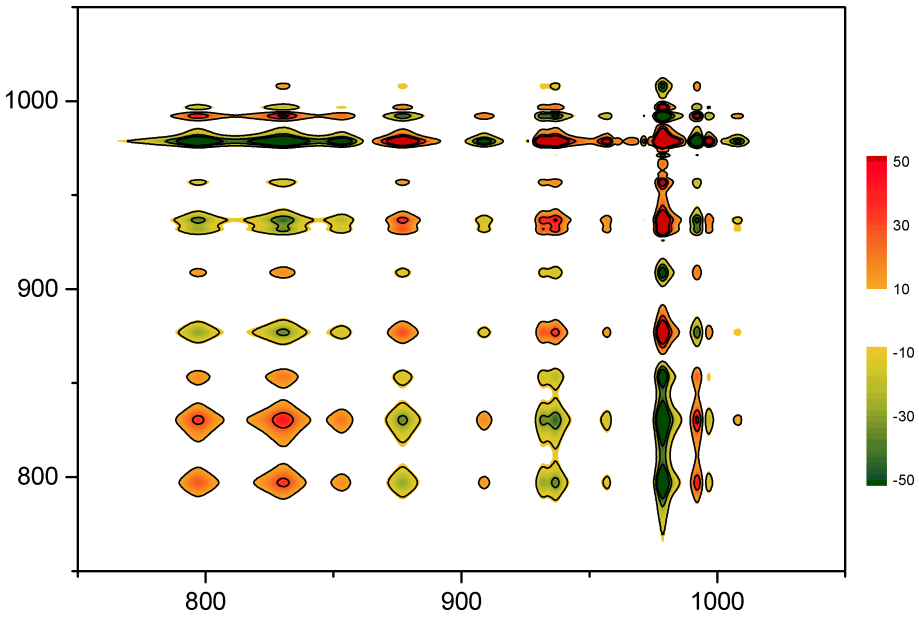

Figure 6: Covariance plot of the 750-1050 cm^{-1} range obtained from the Raman spectra collected during the transition from Re_2O_7 evolving to $Re_2O_7.2H_2O$. Positive correlations appear in red, negative ones in green.

This is definitely confirmed by a multivariate curve resolution -MCR- combined with an alternating least squares -ALS- analysis, which details are provided in Supplementary Materials. The concentration profiles of the two components, namely Re_2O_7 (black line) and $Re_2O_7.2H_2O$ (light green line) afforded by MCR-ALS as a function of time, are presented in Fig. 7.

The cumulative amount of reacted water was evaluated from the integration of μGC data, assuming that the water vapour satisfies the perfect gases' law. The ratio between the molar amount of reacted water and the amount of Re_2O_7, $n = \frac{n(H_2O)}{n(Re_2O_7)}$ shown as a blue line in Fig. 7 spans from zero to 5.3 during the experiment. During the first 5 minutes of reaction, negligible structural evolution is detected, while almost 1 water molecule per Re_2O_7 was adsorbed. In this period, the sorption rate reaches a maximal value of 0.20 mol. of consumed water per mol. of Re_2O_7 per minute. It takes about 7 minutes to have another water molecule per Re_2O_7 adsorbed at the solid, which correlates a 20% conversion of Re_2O_7 to $Re_2O_7.2H_2O$. Between the 15th and 25th minute, the evolution of the share of Re_2O_7 vs. $Re_2O_7.2H_2O$ slows down, and a quasi-plateau where both species are equally present is observed. This phase corresponds to the adsorption of a third water molecule per Re_2O_7 group. After this stage, the share of $Re_2O_7.2H_2O$ gradually increases from 50 to 100% and the water uptake stabilises towards a constant rate of ~0.11 mol. of water per mol. of Re_2O_7 per minute. The relative low rate of phase transition during the first ten minutes of reaction refers to the S-shape evolution of the Johnson-Mehl-Avrami-Kolmogorov (JMAK)

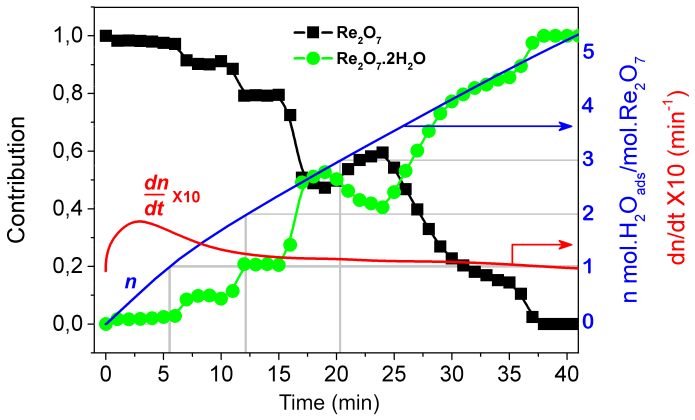

Figure 7: Contribution of Re_2O_7 and $Re_2O_7.2H_2O$ as refined by MCR-ALS analysis plotted together with the ratio n obtained from μ-GC measurements, representing the cumulative molar amount of water uptake per mol. of Re_2O_7 (blue line) and the rate of water uptake, $\frac{dn}{dt}$ (red line).

model. This model aims at describing the nucleation-growth process occurring during phase transitions [28] and has been applied to various evolving systems [29]. According to the JMAK equation, the time evolution of the new phase contribution, denoted as f, can be described by the following expression:

$$f = 1 - e^{-\kappa t^{\alpha}} \tag{1}$$

Where κ is a constant and α is the so-called Avrami exponential factor. In Fig. 8 is plotted the best fit afforded by χ^2 minimization using a Levenberg-Marquadt iterative algorithm together with the experimental evolution and leading to a α value of 2.3. In the present case, nuclei are formed throughout

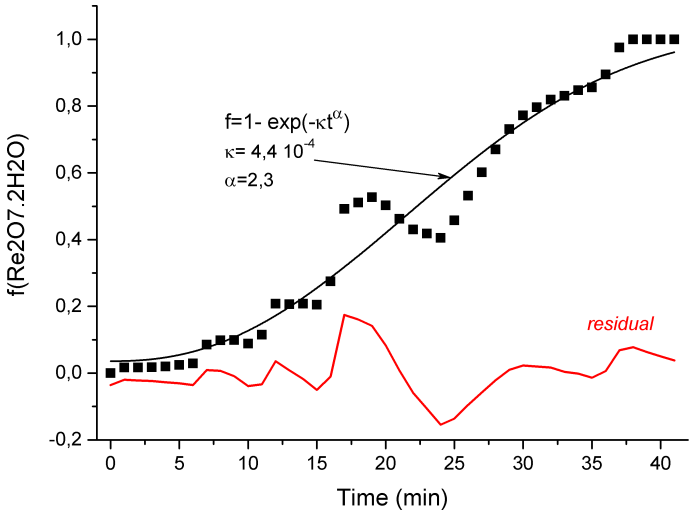

Figure 8: Black squares: fraction of $Re_2O_7.2H_2O$ formed in the course of the controlled hydration, black line: JMAK model curve (see text for details) and red line: residual

the water adsorption, which supports a continuous nucleation process. Following the Avrami model, it is generally admitted that a α value close to 2 suggests a low-dimension (typically mono- or bidimensional) growth model, as occurs when the nucleation sites are non-randomly distributed. This trend makes sense, as the phase transition involves of breaking Re-O-Re bonds in the (xz) cut plane to yield the lamellar

organisation of $Re_2O_7.2H_2O$.

Once the phase transition is completed, at t = 40 min, the molar ratio $n = \frac{n(H_2O)}{n(Re_2O_7)}$ exceeds the nominal value of 2, expected in $Re_2O_7.2H_2O$. Moreover, Fig. 7 shows that for $n \leq 1.8$, almost no structural change is detected, which suggests that a physisorption process precedes the reaction. To make it clear, a corresponding *in situ* experiment was attempted using FTIR spectroscopy in DRIFTS mode. However, as the Re_2O_7 powder tends to pack down during the phase transition, the quality of DRIFTS signal was severely depreciated after 25 minutes of reaction. Because of the lower spectral resolution of IR spectrometer, the 750-1050 cm^{-1} range of the DRIFT spectra presented in Fig. 9 is far less illustrative than what was observed using Raman spectroscopy. Moreover, the fall of signal quality explained above allowed the collection of only few spectra corresponding to $Re_2O_7.2H_2O$. At early stage of reaction (0-15 min), only minor spectral changes can be detected in the 750-1050 cm^{-1} range of the DRIFT spectra presented in Fig. 9, which mainly consist of band broadening. On the other hand, both the 1400-1600 cm^{-1} and the 3000-3600 cm^{-1} regions clearly reflect the rapid formation of a layer of physisorbed molecular water covering the surface of the solid at the very beginning of the process. The values reached by the Kubelka-Munk function largely exceed the linear dependence between the as-measured absorbance and water content, however the shape of the evolution of absorbance as a function of time is shown in Fig. 9, right panel, to illustrate this Langmuir-like adsorption. The latter shows a rapid increase of physisorbed water during the first 10 minutes of hydration, followed by a plateau between t = 10 min and t = 20 min. After 25 minutes under reaction feed, the 600-1100 cm^{-1} spectral region is abruptly modified (Fig. 9, left), while the amount of physisorbed water undergoes another step-wise increase (Fig. 9, right).

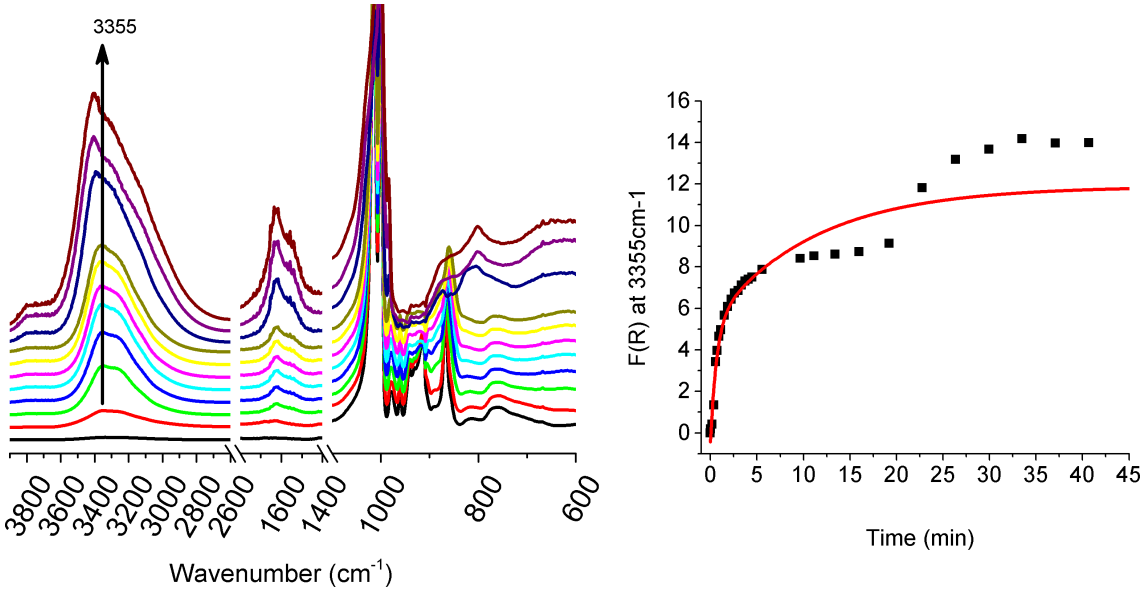

Figure 9: Left: From bottom to top: DRIFT spectra recorded during the first 40 minutes of Re_2O_7 to $Re_2O_7.2H_2O$ reaction; the spectra are shifted vertically for clarity. Right: temporal evolution of the absorbance at 3355 cm^{-1}.

The results presented here make it clear that the interaction of Re_2O_7 with gaseous water firstly consists in the condensation of a film of physisorbed water covering the surface of Re_2O_7. Quickly after the start of this induction period, the conversion of Re_2O_7 to$Re_2O_7.2H_2O$ starts, until reaching one half (Raman), as the amount of physisorbed water stabilizes, as revealed by the DRIFTS experiment (Fig. 9 right panel). This step is followed by a relative structural stability, as both Re_2O_7 and $Re_2O_7.2H_2O$

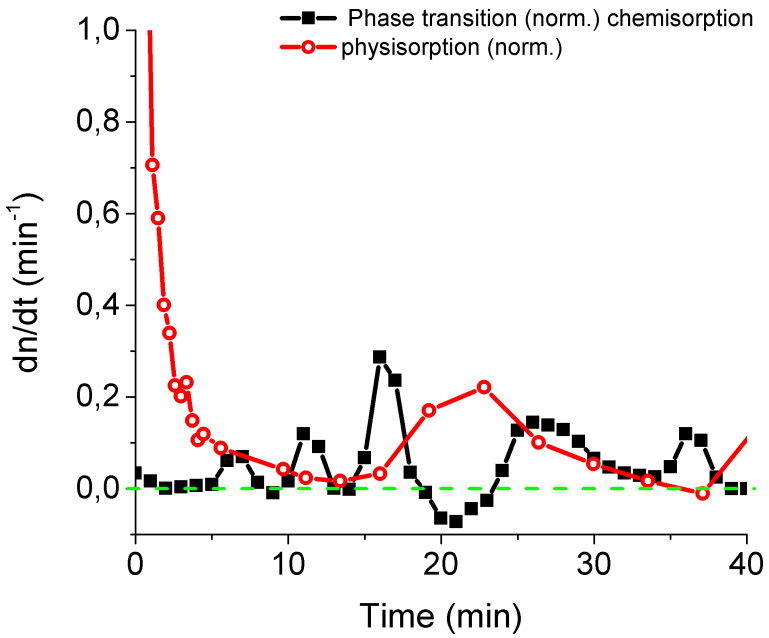

Figure 10: Compared rate tendencies of physisorption and chemisorption processes as a function of time.

are detected in relatively stable extents. In an attempt to look at this plateau more in details, we have compared the molar amount of physisorbed water per mol. of Re_2O_7, denoted as $n_{phys.}$ and estimated from DRIFTS data, with the molar amount of reacted water per mol. of Re_2O_7, denoted as $n_{chem.}$ and obtained from MCR analysis of Raman evolution. Having in mind neither DRIFTS nor Raman can provide a direct quantitative estimation, we have normalised the sum $n_{phys.}+n_{chem.}$ regarding the maximal n value afforded by μ-GC, while considering that, once the phase transition is complete, $n_{chem.}$=2. Accordingly, Fig. 10 displays the trends followed by the rate of water chemisorption $\frac{dn_{chem.}}{dt}$ estimated from MCR analysis of Raman spectra (black line + squares) together with the one of physisorption $\frac{dn_{phys.}}{dt}$ (red line + circles). It is clear from Fig. 10 that the physisorption process precedes the phase transition. At half of the phase transition, our results suggest a pause in the phase transition, which is plausibly accompanied by a boost of physisorption, followed by the further completion of the phase transition.

Conclusions

A crystal of $Re_2O_7.2H_2O$ was prepared by means of a controlled hydration of anhydrous Re_2O_7 at room temperature and was characterized by Raman and XAS spectroscopies. During the hydration-induced phase transition, the adsorption of subsequent amounts of molecular water at the surface of the solid was found to precede the phase transition towards the bis-aquo adduct $Re_2O_7.2H_2O$. From our results, a water coverage corresponding to 2 water molecule per Re_2O_7 is required to produce enough $Re_2O_7.2H_2O$ nuclei for initiating the nucleation of $Re_2O_7.2H_2O$ crystals. Moreover, the phase transition from Re_2O_7 to $Re_2O_7.2H_2O$ follows a S-shape evolution, with a relative stabilisation at half of the process. A refinement supported by the Avrami model suggested that the nucleation sites are localised within a low-dimension space, *e.g.* a surface. Moreover, we found that of the 6.5 water molecules per Re_2O_7 unit needed to get the complete phase transition, 2 are physisorbed before the growth of $Re_2O_7.2H_2O$ and 2 more are physisorbed as both phases co-exists equally.

Keywords

Raman spectroscopy, aqueous adduct, rhenium oxide, in situ, hydration

References

[1] L. Hu, Y. Liu, X. Fang, Y. Zheng, R.-z. Liao, M. Li and Y. Xie, *ACS Catal.*, 2022, **12**, 5857–5863.

[2] A. Müller, B. Krebs and O. Glemser, *Naturwissenschaften*, 1965, **52**, 55–55.

[3] B. Krebs, A. Müller and H. Beyer, *Chem. Commun.*, 1968, 263–264.

[4] B. Krebs, A. Müller and H. H. Beyer, *Inorg. Chem.*, 1969, **8**, 436–443.

[5] I. Beattie and G. Ozin, *J. Chem. Soc. A*, 1969, 2615–2619.

[6] J. Moulijn and J. Mol, *J. Molec. Catal.*, 1988, **46**, 1–14.

[7] D. S. Kim and I. Wachs, *J. Catal.*, 1993, **141**, 419–429.

[8] H. S. Lacheen, P. J. Cordeiro and E. Iglesia, *J. Am. Chem. Soc.*, 2006, **128**, 15082–15083.

[9] M. Stoyanova, U. Rodemerck, U. Bentrup, U. Dingerdissen, D. Linke, R.-W. Mayer, H. L. Rotgerink and T. Tacke, *Appl. Catal. A: General*, 2008, **340**, 242–249.

[10] J. C. Mol, *Catal. Today*, 1999, **51**, 289–299.

[11] R. Toreki and R. R. Schrock, *J. Am. Chem. Soc.*, 1990, **112**, 2448–2449.

[12] M. Chabanas, A. Baudouin, C. Copéret and J.-M. Basset, *J. Am. Chem. Soc.*, 2001, **123**, 2062–2063.

[13] B. Mitra, X. Gao, I. E. Wachs, A. Hirt and G. Deo, *Phys. Chem. Chem. Phys.*, 2001, **3**, 1144–1152.

[14] X. Sécordel, A. Tougerti, S. Cristol, C. Dujardin, D. Blanck, J.-C. Morin, M. Capron, A.-S. Mamede, J.-F. Paul, M.-A. Languille *et al.*, *C. R. Chim.*, 2014, **17**, 808–817.

[15] X. Secordel, E. Berrier, M. Capron, S. Cristol, J.-F. Paul, M. Fournier and E. Payen, *Catal. Today*, 2010, **155**, 177–183.

[16] F. Schekler-Nahama, O. Clause, D. Commereuc and J. Saussey, *Applied Catalysis A: General*, 1998, **167**, 247–256.

[17] A. Yoboué, A. Susset, A. Tougerti, D. Gallego, S. V. Ramani, M. Kalyanikar, D. S. Dolzhnikov, S. G. Wubshet, Y. Wang, S. Cristol and J.-F. c. Paul, *Chem. Commun.*, 2011, **47**, 4285–4287.

[18] G. Brauer and G. Sleater, *Angew. Chem.*, 1966, **78**, 336–336.

[19] H. Beyer, O. Glemser and B. Krebs, *Angew. Chem. Int. Ed.*, 1968, **7**, 295–296.

[20] C. C. Romão, F. E. Kühn and W. A. Herrmann, *Chem. Rev.*, 1997, **97**, 3197–3246.

[21] F. E. Kühn and W. A. Herrmann, in *Metal-Oxo and Metal-Peroxo Species in Catalytic Oxidations*, Springer, 2000, pp. 213–236.

[22] K. Ulbricht and H. Kriegsmann, *Z. Chem.*, 1967, **7**, 244–245.

[23] D. Vantelon, P. Lagarde, A. M. Flank, E. Berrier, X. Secordel, S. Cristol, C. L. Fontaine, F. Villain and V. Briois, *Phase Transit.*, 2009, **82**, 322–335.

[24] G. Wltschek, I. Svoboda and H. Fuess, *Z. anorg. allg. Chemie*, 1993, **619**, 1679–1681.

[25] T. Ferré, T. Cavignac, S. Jobic and C. Latouche, *Comp. Mater. Sci.*, 2023, **228**, 112323.

[26] J. J. Rehr, J. J. Kas, F. D. Vila, M. P. Prange and K. Jorissen, *Phys. Chem. Chem. Phys.*, 2010, **12**, 5503–5513.

[27] M. Gafurov, A. Aliev and I. Akhmedov, *Spectrochim. Acta A*, 2002, **58**, 2683–2692.

[28] C. Kongmark, R. Coulter, S. Cristol, A. Rubbens, C. Pirovano, A. Löfberg, G. Sankar, W. van Beek, E. Bordes-Richard and R.-N. Vannier, *Cryst. Growth Des.*, 2012, **12**, 5994–6003.

[29] K. Shirzad and C. Viney, *J. R. Soc. Interface*, 2023, **20**, 20230242.

TOC entry

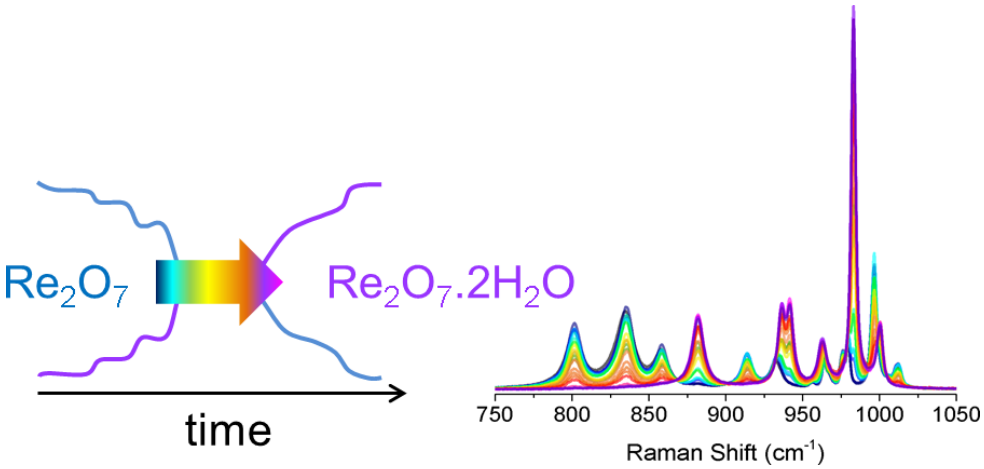

When subjected to ambient conditions, Re_2O_7 rapidly turns into a drop of aqueous $ReO_4^-{}_{aq.}$. By finely controlling the hydration of Re_2O_7, we could obtain and confirm the structure of $Re_2O_7.2H_2O$ as intermediate species with input from DFT modelling. Moreover, we provide here a comprehensive investigation of the Re_2O_7 to $Re_2O_7.2H_2O$ phase transition using *in situ* spectroscopies.